A Novel Mirror Diversity Receiver for Indoor MIMO Visible Light Communication Systems

Ki-Hong Park, Wael G. Alheadary, and Mohamed-Slim Alouini

Computer, Electrical, and Mathematical Sciences and Engineering (CEMSE) Division

King Abdullah University of Science and Technology (KAUST)

Thuwal, Makkah Province, Kingdom of Saudi Arabia

Email: {kihong.park, wael.headary, slim.alouini}@kaust.edu.sa

Abstract

In this paper, we propose and study a non-imaging receiver design reducing the correlation of channel matrix for indoor multiple-input multiple-output (MIMO) visible light communication (VLC) systems. Contrary to previous works, our proposed mirror diversity receiver (MDR) not only blocks the reception of light on one specific direction but also improves the channel gain on the other direction by receiving the light reflected by a mirror deployed between the photodetectors. We analyze the channel capacity and optimal height of mirror in terms of maximum channel capacity for a 2×2 MIMO-VLC system in a 2-dimensional geometric model. We prove that this constructive and destructive effects in channel matrix resulting from our proposed MDR are more beneficial to obtain well-conditioned channel matrix which is suitable for implementing spatial-multiplexing MIMO-VLC systems in order to support high data rate.

I. Introduction

Visible light communication (VLC) has attracted a lot of attention with the rise of the emerging solid-state lighting such as light-emitting diode (LED) and laser diode (LD) to replace the conventional lighting sources thanks to their high efficiency and low cost [1]. Since it is natural to deploy multiple lighting sources at intervals in the ceiling, multiple-input multiple-output (MIMO) indoor VLC systems have gained growing interest in order to support higher data rates

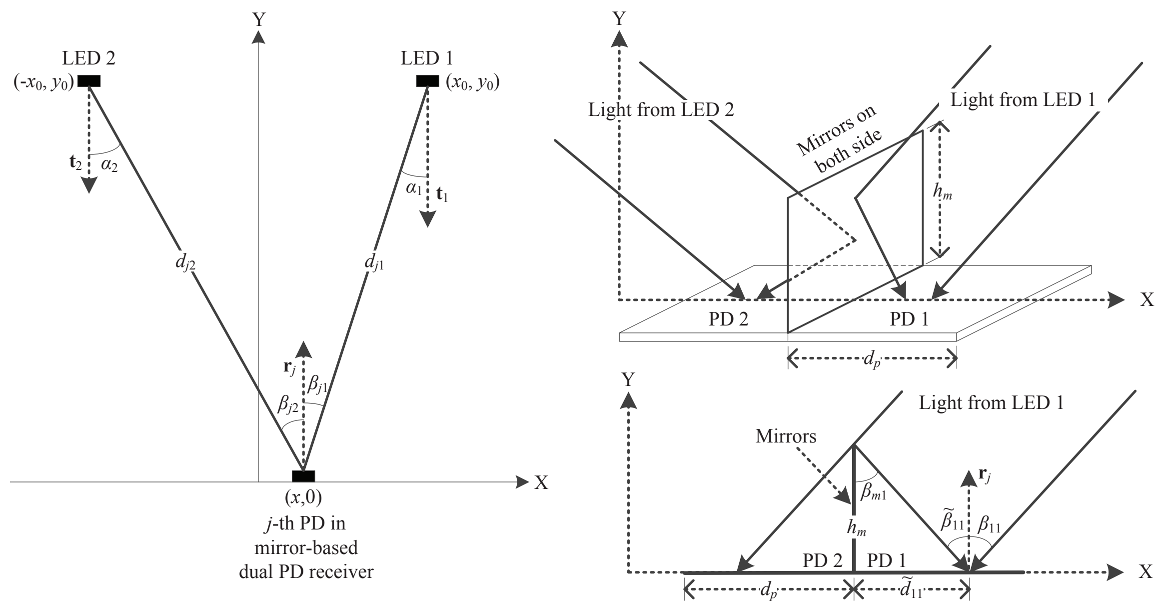

Fig. 1. System model of a 2-dimensional 2×2 OWC-MIMO link equipped with the proposed mirror diversity receiver; The geometry of transmitter-receiver pair (left), the structure of proposed MDR (top right), and the example for its reception of incident light from the 1st LED with $\mathbf{r}_j = [0\ 1]^T$ (bottom right).

by transmitting different information streams from different lighting sources [2]. However, it is difficult to apply spatial-multiplexing MIMO scheme in indoor VLC intensity channel with a dominant line-of-sight (LoS) link because it results in highly correlated channel matrix preventing from decoding the received signals in parallel at the receiver.

In order to reduce the correlation between the channel vectors in matrix, various advanced receiver structures have been proposed. Recently, some papers have considered the imaging receivers using the lenses such as convex lens, hemispherical lens, and fisheye lens [3]–[5]. A lens is used to project the optical intensity signals on the receiver photodetector (PD) array with partial and complete separated light images which result in well-conditioned channel matrix. However, the imaging receivers with a lens results in some disadvantages such as a limited field-of-view (FoV), a limitation of receiver size and the necessity of additional optics depending on the type of lens.

On another front, non-imaging receivers have been proposed to reduce the channel correlation. Line-blocked receiver (LBR) is a simple and efficient method to reduce the correlation by blocking the specific link from an LED to a PD [6] but is difficult to practically implement by adaptively reflecting the change of blocking area due to the user mobility and location. Another simple method called spatially-separated receiver (SSR) is to separate the PDs at the receiver to reduce the correlation by making larger difference between the transmission distances and between the incident angles of light on arrival at PDs [6]. It is practical to implement but makes the receiver size larger and provides limited performance enhancement. Recent papers have also considered an advanced receiver making less-correlated channels by reducing the channel gains from the specific direction [7], [8]. In [7], the angle diversity receiver (ADR) has been proposed to vary the orientation angles of PDs so that the incident light from the specific direction can not reach the receiver plane or is directed out of the receiver FoV. The prism array receiver (PAR) in [8] deploys a prism on the top of each PD plane to orient the specific direction. Therefore, only the light oriented toward the specific direction can pass through the prism and reach the receiver PD plane.

Most of the MIMO-VLC non-imaging receivers except SSR addressed here focused on destructing the channel gains from specific LED-to-PD links in order to reduce the correlation. In other words, these receivers end up with the spatial directivity for each PD by blocking or interfering with the reception of intensity signals in the specific direction. Unlike previous receivers only utilizing the destructive impact by introducing directivity, we propose in this paper a new receiver design which exploits both destructive and constructive effect on directivity at the receiver. In order to reduce the correlation, our proposed mirror diversity receiver (MDR) deploys both-side mirrors between the PDs which can help destructively reduce the channel gains from specific direction by block the light as well as constructively increase the channel gain from another directions by receiving the reflective lights at PD.[1] We analyze the performance of 2×2 MIMO-VLC system in two-dimensional geometric model. We verify the superiority over previous non-imaging receiver in terms of capacity and also investigate the optimal height of the mirror to maximize the channel capacity. Finally, we discuss the extension of our proposed MDR to general MIMO-VLC system and the applicability along with the previous non-imaging receivers.

The remainder of this paper is organized as follows. Section II introduces the system model for the two-dimensional 2×2 MIMO-VLC. Our proposed MDR is described in details in Section

---

[1] Any reflectors can be replaced with mirrors for the same purpose.

III and analyzed in Section IV. Numerical results in Section V validate the superiority of the proposed MDR. Finally, a brief conclusion summarizing the main results and discussing future works of the paper are given in Section VI.

II. System Model

In this paper, we consider as shown in Fig. 1 an optical wireless communication MIMO system where the transmitter is equipped with two LEDs and the proposed receiver is equipped with two PDs. We consider an intensity modulation and direct detection (IM-DD) scheme for modulation and demodulation in this system. As you can see in the figure, it is assumed that there only exists direct line-of-sight (LoS) link and we do not consider the reflections. For simplicity, we assume that the transmitter-receiver pair is aligned in the two-dimensional cartesian coordinate while we note that our proposed receiver can be easily extended to three-dimensional space. Each LED is symmetrically located over X-axis and in the same height in Y-axis, i.e., the i-th LED is on the point $((3-2i)x_0, y_0)$, where $x_0 > 0$ and $y_0 > 0$. Each LED irradiates the light in the Lambertian radiation pattern centered in the direction of unit vector $\mathbf{t}_i$. We assume that the receiver size is relatively small compared to the transmission distance and two PDs are co-located on the point $(x, 0)$, that is, it is assumed that the transmission distances and the irradiance angles between the i-th LED and both PDs are the same, i.e., $d_{1i} = d_{2i} = d_i$ and $\alpha_{1i} = \alpha_{2i} = \alpha_i$. We note that the j-th PD plane is oriented in the direction of unit vector $\mathbf{r}_j$.

Each electrical signal is modulated for the input of each LED, converted to the intensity signal s_i for $i = 1, 2$. At the receiver, each PD fulfills direct detection to an electrical current signal y_j for $j = 1, 2$ proportionally to the received intensity signal. For the sake of simplicity, the received signal can be represented in vector space as

$$\mathbf{y} = \mathbf{H}\mathbf{s} + \mathbf{n}, \tag{1}$$

where $\mathbf{n} = [n_1 \;\; n_2]^T$ denotes independent and identically distributed (i.i.d.) additive white Gaussian noise (AWGN) vectors with zero mean and variance of $\sigma_{n_j}^2 = \frac{N_0}{2}$.[2] $\mathbf{H} \in \mathbb{R}^{2\times 2}$ is the 2×2 channel matrix whose element h_{ji} represent the channel gain between the i-th LED

[2]We note that the shot and thermal noise in receiver electric domain are generally modeled as AWGN.

and the j-th PD which is given by

$$h_{ji}=\frac{(m+1)A_{ji}}{2\pi d_{ji}^2}\cos^m\alpha_{ji}\cos^k\beta_{ji},\ |\alpha_{ji}|\leq\frac{\pi}{2},|\beta_{ji}|\leq\frac{\mathrm{FoV}}{2}, \tag{2}$$

and $h_{ji}=0$, otherwise. Here, α_{ji}, β_{ji}, d_{ji} and A_{ji} are the irradiance angle at the i-th LED to the receiver, the incident angle at the j-th PD from the i-th LED, the transmission distance between the i-th LED and j-th PD and the active area of the j-th PD with respect to the i-th LED. Each angle can be computed as

$$\cos\alpha_{ji} \ = \ \mathbf{d}_{ji}\cdot\mathbf{t}_i \tag{3}$$

$$\cos\beta_{ji} \ = \ -\mathbf{d}_{ji}\cdot\mathbf{r}_j, \tag{4}$$

where $\mathbf{d}_{ji}$ denotes the direction vector from the i-th LED to the j-th PD which is given by $\mathbf{d}_{ji}=\frac{[x-(3-2i)x_0 \ \ -y_0]^T}{d_{ji}}$. k denotes the FoV coefficient of the PD and the Lambertian emission order is given as

$$m=\frac{-\ln 2}{\ln(\cos\Phi_{\frac{1}{2}})}, \tag{5}$$

where $\Phi_{\frac{1}{2}}$ denotes the semi-angle at half-power of light emission in LED. In the conventional non-imaging receiver using the PDs with the same PD plane size, the active area of PDs for each channel element is the same as A. Due to the high correlation between channel vectors with respect to two LEDs, it prevents from utilizing spatial multiplexing MIMO transmission and decoding in the conventional receiver. In the next section, we propose a new receiver structure to reduce the correlation by deploying a mirror between two PDs.

III. Proposed Mirror Diversity Receiver

In the top right of Fig. 1, we present the structure of the proposed MDR. In order to obtain the channel vectors having lower correlation, our main idea is to deploy the both-side mirror perpendicularly to the X-axis between two PDs. Depending on the oriented direction of incident light, each PD can receive more light intensity due to the reflective light by mirror, while, at the same time, the incident light from the other direction is blocked by the mirror. By doing so, each PD can exploit the spatial directivity to successfully separate the intensity signal of one LED from that of the other LED. For example as shown in the bottom right of Fig. 1, the first PD gains more light intensity by reflective light from the mirror, while the second PD has the shaded plane not receiving the light from the first LED due to the blockage of the mirror. Now we can compute the additional channel gain and the loss of channel gain due to the mirror to find the channel matrix at the proposed MDR. We only analyze the channel matrix in the range of $x \geq 0$ due to the symmetry. We assume that the active area of two PDs is in the shape of square with the same area $A = d_p^2$, where d_p is the length of one side. The height of mirror is defined as h_m. Depending on the location of the LED relative to the location of receiver, we know that the channel gain of each PD increases or decreases. Considering two scenarios in which the receiver can be located, i.e., between two LEDs, $0 \leq x < x_0$ or outside of two LEDs, $x \geq x_0$, we can calculate the channel matrix at the proposed MDR.

A. *Scenario 1:* $0 \leq x < x_0$

The received intensity through direct LOS link without the mirror can be already obtained by (2) and we focus on the amount of received intensity or loss of intensity due to the mirror. As you can see in Fig. 1, in this scenario, the i-th PD can gather more reflective light from the i-th LED, while it loses some amount of intensity from the other LED due to the blockage of mirror. The increased and decreased amount of intensity is proportional to the effective active-area at each PD which can gather the reflective light or can be shaded by the mirror. In order to calculate the effective active-area receiving extra reflective light, we first calculate the incident angles of light into the mirror and reflective light into the PD plane which is given by

$$\begin{aligned} \cos\beta_{mj} &= -\mathbf{d}_{jj} \cdot [0\ 1]^T \\ \cos\tilde{\beta}_{jj} &= -(\mathbf{T}_m \mathbf{d}_{jj}) \cdot \mathbf{r}_j, \end{aligned} \tag{6}$$

where $\mathbf{T}_m$ denotes the transformation matrix due to the mirror which is given by $\mathbf{T}_m = \left[\begin{smallmatrix} -1 & 0 \\ 0 & 1 \end{smallmatrix}\right]$. As shown in the bottom right of Fig. 1, let us define the effective maximum length of one side as $\tilde{d}_{ji}$ in PD plane which the reflective light can reach in the case of $i = j$ or be blocked in the case of $i \neq j$. It can be computed by using the trigonometric identities as

$$\tilde{d}_{ji} = \begin{cases} \min\left(\dfrac{h_m \sin\beta_{mi}}{\cos\tilde{\beta}_{ii}}, d_p\right), & i = j \\ \min\left(\dfrac{h_m \sin\beta_{mi}}{\cos\tilde{\beta}_{ji}}, d_p\right), & i \neq j. \end{cases}, \tag{7}$$

where we note that we use the identity of $\tilde{\beta}_{ji} = \beta_{ji}$ in case of $i \neq j$ for notational simplicity. Now the effective active-area where receives the reflective light or be shaded can be calculated

$$\tilde{h}_{ji} = \begin{cases} h_{ji} + (-1)^{i+j}\eta_m^{\delta_{j-i}} \frac{(m+1)\tilde{A}_{ji}}{2\pi d_{ji}^2} \cos^m \alpha_{ji} \cos^k \tilde{\beta}_{ji}, & \text{if } |\alpha_{ji}| \le \frac{\pi}{2},\ |\beta_{ji}| \le \frac{\text{FoV}}{2}, |\tilde{\beta}_{ji}| \le \frac{\text{FoV}}{2} \\ h_{ji}, & \text{if } |\alpha_{ji}| \le \frac{\pi}{2},\ |\beta_{ji}| \le \frac{\text{FoV}}{2}, |\tilde{\beta}_{ji}| > \frac{\text{FoV}}{2} \end{cases} \quad (8)$$

$$\tilde{h}_{ji} = \begin{cases} h_{ji} + (-1)^{j}\eta_m^{\delta_{j-2}} \frac{(m+1)\tilde{A}_{ji}}{2\pi d_{ji}^2} \cos^m \alpha_{ji} \cos^k \tilde{\beta}_{ji}, & \text{if } |\alpha_{ji}| \le \frac{\pi}{2},\ |\beta_{ji}| \le \frac{\text{FoV}}{2}, |\tilde{\beta}_{ji}| \le \frac{\text{FoV}}{2} \\ h_{ji}, & \text{if } |\alpha_{ji}| \le \frac{\pi}{2},\ |\beta_{ji}| \le \frac{\text{FoV}}{2}, |\tilde{\beta}_{ji}| > \frac{\text{FoV}}{2} \end{cases} \quad (9)$$

as $\tilde{A}_{ji} = \tilde{d}_{ji} d_p$. Therefore, the overall channel gain at the proposed MDR can be computed as (8) where $\eta_m \in [0, 1]$ denotes mirror reflection coefficient that is equal to one with the only perfect mirror and δ_k is the Dirac delta function where $\delta_k = 1$ for $k = 0$ and $\delta_k = 1$ otherwise. We observe from (8) that the channel gains of diagonal components in the channel matrix are increased compared with that at the conventional receiver, while that of off-diagonal components are reduced. It means that the two channel vectors for the first and second LED can be further uncorrelated by introducing our proposed MDR.

B. Scenario 2: $x \ge x_0$

It is clear to see that some of the intensity signals from both LEDs are blocked at the first PD due to the mirror, while the reflected intensity signals by mirror can help increase the channel gain at the second PD. Similarly to the previous section, we can calculate the channel gain which is given by (9). As you can see, when $j = 1$, the channel gains in the first row in the channel matrix is reduced compared to that at the conventional receiver. On the other hand, when $j = 2$, the channel gains in the second row in the channel matrix is increased.

C. Relation to Previous Receivers

We can observe that some of the previous receiver structure can be the special cases of our proposed MDR by adjusting the system parameters taken into consideration to calculate the channel matrix. For example, we know that the proposed MDR without mirror ($h_m = 0$) is the same as some types of conventional receivers. In Table. I, we summarize the relation between the type of receivers and the corresponding system parameters.

TABLE I. RELATION TO VARIOUS RECEIVERS

Type of Receivers	System Parameters	
	Height of mirror	Incident vector of PD
Conventional receiver	$h_m = 0$	$\mathbf{r}_j = [0\ 1]^T,\ \forall j$
Pyramid ADR [7]	$h_m = 0$	$\mathbf{r}_j = \mathbf{T}_m \mathbf{r}_i$
Hemispheric ADR [7]	$h_m = 0$	$-^\dagger$
Pure MDR	$h_m > 0$	$\mathbf{r}_j = [0\ 1]^T,\ \forall j$
Combined MDR-ADR	$h_m > 0$	$-^\dagger$

†Any unit vectors

$$\tilde{h}_{ji} = \begin{cases} \dfrac{(m+1)}{2\pi d_i^2} \cos^m \alpha_i \cos^k \beta_i \left(A + (-1)^{i+j} \eta_m^{\delta_{j-i}} d_p \tilde{d}_i \right), & \text{if } |\alpha_i| \le \frac{\pi}{2},\ |\beta_i| \le \frac{\text{FoV}}{2},\ 0 \le x < x_0 \\ \dfrac{(m+1)}{2\pi d_i^2} \cos^m \alpha_i \cos^k \beta_i \left(A + (-1)^{j} \eta_m^{\delta_{j-2}} d_p \tilde{d}_i \right), & \text{if } |\alpha_i| \le \frac{\pi}{2},\ |\beta_i| \le \frac{\text{FoV}}{2},\ x \ge x_0 \end{cases} \quad (10)$$

As you can see in Table I, we note that our proposed MDR can be applied together with previous advanced-receivers. In addition, unlike the LBR or SSR, our proposed receiver does not make the challenging issues such as sensitivity to the receiver mobility/location and limitation to the receiver size to implement the spatially separated PDs.

IV. Performance Analysis of Mirror Diversity Receiver

In this section, we analyze the performance of our proposed pure MDR to check the superiority of our proposed receiver compared with the other receiver. Therefore, we assume that we set the incident vector of PD to $\mathbf{r}_j = [0\ 1]^T$. With this assumption, we note that the following identities holds; $\beta_{mj} = \tilde{\beta}_{jj} = \beta_{ij} \triangleq \beta_j$ for $i \neq j$. For simplicity, using $A_{ji} = A$, $d_{ii} = d_{ji} \triangleq d_i$, and $\alpha_{ii} = \alpha_{ji} \triangleq \alpha_i$, the channel gain at the pure MDR can be computed as (10), where $\tilde{d}_i = \min(h_m \tan \beta_i, d_p)$ can be easily computed by manipulating (7) and defining $\tilde{d}_{ii} = \tilde{d}_{ji} \triangleq \tilde{d}_i$. As you can observe in (10), it is the worst-case scenario for the conventional receiver ($h_m = 0$) to use the spatial multiplexing MIMO. This is because two transmit intensity signals from the first and the second LED are the scaled signals that are perfectly overlapped in the same direction vector of $[1/\sqrt{2}\ 1/\sqrt{2}]^T$ and it cannot decode two transmit signals. For simplicity, let us define the indicator function to check if the incident angle of light falls into the range of receiver FoV, i.e.,

$$u_i = \begin{cases} 1, & \text{if } |\beta_i| \le \frac{\text{FoV}}{2} \\ 0, & \text{if } |\beta_i| > \frac{\text{FoV}}{2} \end{cases} . \tag{11}$$

Letting $\xi_i \triangleq \frac{(m+1)}{2\pi d_i^2} \cos^m \alpha_i \cos^k \beta_i u_i$ and the element of effective active-area matrix $\tilde{\mathbf{A}}$

$$\tilde{A}_{ji} = \begin{cases} A + (-1)^{i+j} \eta_m^{\delta_{j-i}} d_p \tilde{d}_i, & \text{if } 0 \le x < x_0 \\ A + (-1)^j \eta_m^{\delta_{j-2}} d_p \tilde{d}_i, & \text{if } x \ge x_0 \end{cases} ,$$

the channel matrix at the pure MDR can be represented as

$$\tilde{\mathbf{H}} = \tilde{\mathbf{A}} \text{diag}(\xi_1, \xi_2), \tag{12}$$

where $\text{diag}(\xi_1, \xi_2)$ denotes the diagonal matrix consisting of the elements ξ_1 and ξ_2. For conventional receiver with $h_m = 0$, the effective active-area matrix is $\tilde{\mathbf{A}} = A\mathbf{1}\mathbf{1}^T$ and the rank of the channel matrix is $\text{rank}(\mathbf{H}) = \text{rank}(A\mathbf{1}\mathbf{1}^T \text{diag}(\xi_1, \xi_2)) = 1$. Again, it proves that the conventional receiver cannot support multiplexing MIMO in this worst-case scenario. On the other hand, the channel matrix at the proposed MDR ($h_m > 0$) consists of product of two rank-two matrices of $\tilde{A}$ and $\text{diag}(\xi_1, \xi_2)$ and can support multiplexing MIMO.

A. *Channel Capacity*

First we consider the channel capacity of the MIMO system with the known channel state information (CSI) at the receiver only. When the average electrical SNR at the transmitter is constrained on $\mathbb{E}[\|\mathbf{s}\|^2] = P$ and the power is equally allocated to each LED, the channel capacity can be computed as[3]

$$C = \frac{1}{2} \log_2 \det \left| \mathbf{I} + \rho \tilde{\mathbf{H}} \tilde{\mathbf{H}}^T \right|, \tag{13}$$

---

[3]It is the capacity formula in the classical MIMO system, while the channel capacity upper and lower bounds in optical wireless intensity channel are obtained in [9, Eq. (7.43)]. We note that the above capacity formula is enough to verify the performance of various receivers because 1) it is also used in the previous literature [7], [10] and references therein for performance comparison and evaluation in optical wireless intensity channel; and 2) it is in the same form as the achievable rate formula of constant power and continuous rate adaptation optical MIMO systems in [11, Eq. (24)-(25)] by introducing the bit error rate requirement.

where $\rho \triangleq \frac{P}{N_0}$ is the average electrical SNR per LED. Using (12), it can be rewritten as

$$
\begin{aligned}
C &= \frac{1}{2}\log_2 \prod_{m=1}^{2} (1+\rho\lambda_m) \\
&= \frac{1}{2}\log_2 \Big(1+\rho(\xi_1\tilde{A}_{11}+\xi_2\tilde{A}_{22}) \\
&+ \rho^2\xi_1\xi_2(\tilde{A}_{11}\tilde{A}_{22}-\tilde{A}_{12}\tilde{A}_{21})\Big),
\end{aligned} \tag{14}
$$

where λ_m denotes the eigenvalues of the channel matrix $\tilde{\mathbf{H}}\tilde{\mathbf{H}}^T$.

B. Optimal Height of a Perfect Mirror

We note that the capacity depends on the height of mirror h_m and can be maximized with optimal h_m. For analysis, we here assume a perfect mirror, i.e., $\eta_m = 1$.

Theorem 1 (Optimal Height of Mirror): The channel capacity of 2×2 MIMO-VLC two-dimensional systems with the pure MDR with perfect mirror is maximized with the optimal height of mirror as follows. For $0 \le x < x_0$,

$$h_m^* \ge \frac{d_p}{\tan\beta_1}. \tag{15}$$

For $x \ge x_0$,

$$\begin{cases} h_m^* \ge \frac{d_p}{\tan\beta_1}, & \text{if } \frac{2\rho A^2\xi_2^2}{1+2\rho A^2\xi_2^2} \le \frac{1}{2}\Big(1+\frac{\tan\beta_1}{\tan\beta_2}\Big) \\ h_m^* = \frac{d_p}{\tan\beta_2}, & \text{otherwise} \end{cases}. \tag{16}$$

Proof: We first consider the case for $0 \le x < x_0$. In this case, we prove that (14) with $\tilde{d}_1 = d_p$ and $\tilde{d}_2 = d_p$, i.e., $h_m \ge \frac{d_p}{\tan\beta_1}$ is always larger than that with the other case of $\tilde{d}_j$ on $h_m < \frac{d_p}{\tan\beta_1}$. The determinant in (13) for $h_m \ge \frac{d_p}{\tan\beta_1}$ defined as $D(\tilde{d}_1, \tilde{d}_2) = \det\left|I+\rho\tilde{\mathbf{H}}\tilde{\mathbf{H}}^T\right|$ can be computed as

$$D(d_p, d_p) = (1+4\rho A^2\xi_1^2)(1+4\rho A^2\xi_2^2). \tag{17}$$

For $\frac{d_p}{\tan\beta_2} \le h_m < \frac{d_p}{\tan\beta_1}$, the following inequality of the determinant holds:

$$
\begin{aligned}
D(h_m\tan\beta_1, d_p) &= (1+2\rho A^2(1+a^2)\xi_1^2)(1+4\rho A^2\xi_2^2) \\
&- (2\rho A^2\xi_1\xi_2(1-a))^2 \\
&< \left(1+4\rho A^2\xi_1^2\frac{1+a^2}{2}\right)(1+4\rho A^2\xi_2^2) \\
&< D(d_p, d_p),
\end{aligned} \tag{18}
$$

where we define $a = \frac{h_m \tan\beta_1}{d_p}$ for $\frac{\tan\beta_1}{\tan\beta_2} \le a < 1$ in this range. Similarly, for $0 \le h_m < \frac{d_p}{\tan\beta_2}$, we can see the following inequality holding:

$$\begin{aligned} &D(h_m \tan\beta_1, h_m \tan\beta_2) \\ &\quad = \left(1 + 4\rho A^2 \xi_1^2 \frac{1+a^2}{2}\right)\left(1 + 4\rho A^2 \xi_2^2 \frac{1+b^2}{2}\right) \\ &\quad - (2\rho A^2 \xi_1 \xi_2 (1-ab))^2 \\ &\quad < D(d_p, d_p), \end{aligned} \tag{19}$$

where we define $b = \frac{h_m \tan\beta_2}{d_p}$ for $0 \le a \le b < 1$ in this range. Therefore, in order to maximize the capacity, the optimal h_m is set to $h_m^* \ge \max\left(\frac{d_p}{\tan\beta_1}, \frac{d_p}{\tan\beta_2}\right) = \frac{d_p}{\tan\beta_1}$ so that $\tilde{d}_1 = d_p$ and $\tilde{d}_2 = d_p$.

We now consider the case for $x \ge x_0$. For $h_m \ge \frac{d_p}{\tan\beta_1}$, the determinant can be calculated as $D(d_p, d_p) = 1 + 4\rho A^2(\xi_1^2 + \xi_2^2)$. For $\frac{d_p}{\tan\beta_2} \le h_m < \frac{d_p}{\tan\beta_1}$, the determinant is given by

$$\begin{aligned} D(h_m \tan\beta_1, d_p) \; &= \; 1 + 2\rho A^2(1+a^2)\xi_1^2 + 4\rho A^2 \xi_2^2 \\ &+ \; (2\rho A^2 \xi_1 \xi_2 (1-a))^2. \end{aligned} \tag{20}$$

We note that $D(h_m \tan\beta_1, d_p) = D(d_p, d_p)$ for $a = 1$. (20) is a convex quadratic function in a variable a. Therefore, the determinant in (20) is maximized at the end of range, i.e., $\max_a D(h_m \tan\beta_1, d_p) = \max(D(h_m \tan\beta_1, d_p)|_{a=\frac{\tan\beta_1}{\tan\beta_2}}, D(h_m \tan\beta_1, d_p)|_{a=1})$. The a-coordinate of vertex in this function is $a_v = \frac{2\rho A^2 \xi_2^2}{1+2\rho A^2 \xi_2^2}$ which ranges in $(0, 1)$. (20) becomes larger as the variable a becomes far away from the a-coordinate of vertex. Therefore, the following inequality holds:

$$D\left(h_m \tan\beta_1, d_p\right)|_{a=\frac{\tan\beta_1}{\tan\beta_2}} \ge D(d_p, d_p) \text{ if } a_v \ge \frac{1}{2}\left(1 + \frac{\tan\beta_1}{\tan\beta_2}\right),$$

while $D\left(h_m \tan\beta_1, d_p\right)|_{a=\frac{\tan\beta_1}{\tan\beta_2}} < D(d_p, d_p)$, otherwise. For $0 \le h_m < \frac{d_p}{\tan\beta_2}$, the determinant in this range is bounded by

$$\begin{aligned} &D(h_m \tan\beta_1, h_m \tan\beta_2) \\ &\quad = 1 + 2\rho A^2(1+a^2)\xi_1^2 + 2\rho A^2(1+b^2)\xi_2^2 \\ &\quad + (2\rho A^2 \xi_1 \xi_2 (b-a))^2 \\ &\quad < 1 + 2\rho A^2(1+a^2)\xi_1^2 + 4\rho A^2 \xi_2^2 + (2\rho A^2 \xi_1 \xi_2 (1-a))^2 \\ &\quad < D\left(h_m \tan\beta_1, d_p\right)|_{a=\frac{\tan\beta_1}{\tan\beta_2}}. \end{aligned} \tag{21}$$

Finally, we can see the optimal $h_m^* = \frac{d_p}{\tan\beta_2}$ or $h_m^* \geq \frac{d_p}{\tan\beta_1}$ under the condition on the vertex described above. ■

For $0 \leq x < x_0$, the capacity is maximized when the non-diagonal elements in the channel matrix become zero. In other words, the capacity is maximized if the light radiated from the j-th LED is perfectly blocked at the i-th PD, while exploiting its reflective intensity signals to enhance the received power at the j-th PD, and vice versa. We also note that the minimum optimal height of mirror is dependent on the incident angle of light from the first LED β_1 which varies on the receiver position in the range. At $x = 0$, β_1 is the largest in the range of $0 \leq x < x_0$ and optimal h_m can be minimized, which means that the optimal pure MDR can be implemented practically. On the other hand, as the receiver position becomes close at $(x_0, 0)$, β_1 approaches zero and therefore optimal h_m approaches infinity, which means that it is practically impossible to implement the optimal pure MDR due to the limitation of receiver size.

For $x \geq x_0$, the channel capacity under the optimal height of mirror depends on the condition that is related to ρ, A and β_j for $j = 1, 2$. For the fixed transmitter/receiver position, when $h_m^* \geq \frac{d_p}{\tan\beta_1}$, the channel matrix is a rank-1 matrix, while the channel matrix with $h_m^* = \frac{d_p}{\tan\beta_2}$ is the rank-two matrix. Therefore, the transmission mode can be changed as follows.

Corollary 1.1: For fixed transmitter and receiver position under $x \geq x_0$, the multiplexing scheme is the optimal transmission mode to achieve the channel capacity in high SNR regime, while the beamforming scheme is the optimal one in the low SNR regime.

V. Numerical Results

In our performance evaluation, we consider the system model in Fig.1 by using the following parameters given in Table II below. We note here that we utilize the mirror with fixed height because it is not optimal at each receiver position but practical to implement adaptively for user mobility and location. In addition, excepting the parameters for the mirror, we use the similar system parameters that the ones used in the simulation in [6], [7]. For comparison, we consider other MIMO-VLC non-imaging receivers, i.e., spatially-separated receiver (SSR), line-blocked receiver (LBR), and angle diversity receiver (ADR). Typical system parameters for LEDs and PDs are the same as mentioned in Table II. The separation between two PDs in SSR is defined as $x_s = 10$ cm and we assume that two PDs at SSR are located at the points $(x \pm \frac{x_s}{2}, 0)$. For LBR, it is assumed that the specific links from the i-th LED to j-th PD for $i \neq j$ are perfectly blocked

TABLE II. SYSTEM PARAMETERS FOR SIMULATION

	Parameters	Values
LED	Location at (x_0, y_0) and $(-x_0, y_0)$	$(2, 3)$ and $(-2, 3)^{\dagger}$
	Direction vector of irradiation in center ($\mathbf{t}_i$)	$[0\ -1]^T$
	Semi-angle at a half power ($\Phi_{1/2}$)	60°
	Lambertian emission order (m)	1
MDR	Location at $(x, 0)$	$x = 0$ to $x = 3$
	Direction vector of PD orientation ($\mathbf{r}_j$)	$[0\ 1]^T$
	Receiver field-of-view (FoV)	180°
	FoV coefficient (k)	1
	Active area of PD (A)	1 cm^2
	Length of one side at PD plane (d_p)	1 cm
	Height of mirror (h_m)	1 cm‡
	Reflection coefficient of mirror (η_m)	0.8‡

†The unit of distance is meter (m).

‡Unless otherwise stated.

to make the channel matrix uncorrelated. Thus, we here assume that non-diagonal elements of channel matrix at LBR are zero, i.e., $h_{ji} = 0$ for all $i \neq j$. For ADR, it is required to find the optimal angle of PD orientation which we numerically obtain to maximize the channel capacity for each receiver position as in [7].

Fig. 2 illustrates the channel capacity of 2×2 MIMO-VLC system with various receivers with respect to the receiver position for different SNRs. Due to the small size of active area in PD, the channel gains $\tilde{h}_{ji}$ (or h_{ji}) in the system are nearly around 60 dB, which means that ρ should be at least 120 dB for reasonable performance.[4] Therefore, we consider three scenarios with $\rho = 120, 140$, and 160 dB. We show from this figure that the proposed MDR outperforms the existing advanced receivers at all the receiver position and SNR of interest. We can see that the constructive effect on the channel gain by receiving the reflective light can further improve the system performance unlike the other receivers only utilizing the destructive effect on the channel gain by blocking the link. For $\rho = 120$ dB which means low received SNR, the performance gap among our proposed MDR and the other receivers is smaller than that in high received SNR regime with $\rho = 160$ dB. We also note that our proposed MDR provides better performance even though we do not use the mirror with optimal height but with fixed height.

[4]We note that this operating SNR range is almost the same as [7], [8].

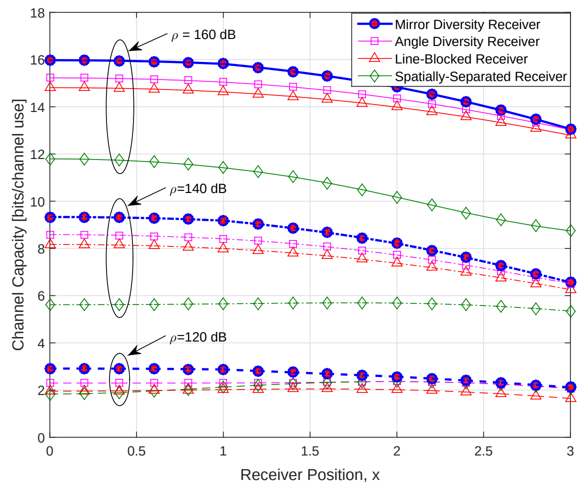

Fig. 2. Channel capacity as a function of the receiver position in SSR, LBR, ADR, and the proposed MDR for different SNRs.

In Fig. 3, we present the channel capacity of the proposed MDR with respect to the height of perfect mirror h_m at different receiver positions, $x = 1$ and $x = 3$. For the arbitrarily chosen SNRs, Fig. 3 verifies the validity of Theorem 1 describing the optimal height of perfect mirror. We also see that the optimal height of perfect mirror in high receive SNR regime is only 6 mm which is smaller than d_p. It means that the optimal pure MDR can be compactly implemented. Moreover, we note that there exists the trade-off between the system performance and the implementation cost (height of mirror) when $x < x_0$.

VI. Conclusions and Future Works

In this paper, we proposed a new non-imaging receiver structure utilizing both-side mirror in order to enhance the system performance by interfering the reception of the light in one specific link as well as by enhancing the reception of light in another specific link. Our proposed MDR can further provide lower correlation of channel matrix while enhancing the channel gain itself. We analyzed and verified our proposed MDR for a two-dimensional 2×2 MIMO-VLC system by comparing it with existing non-imaging receivers. Finally, we found the optimal height of perfect mirror maximizing the channel capacity of MIMO-VLC system utilizing our proposed MDR. Although we consider the specific MIMO-VLC system in two-dimensional geometric model, we note that our numerical results is enough to prove that the proposed MDR is the

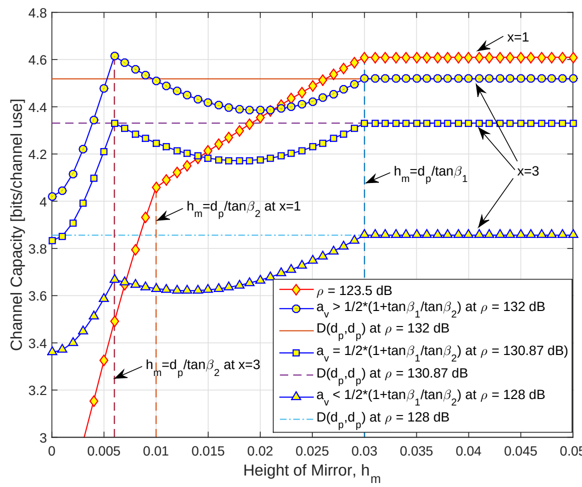

Fig. 3. Channel capacity of the proposed MDR as a function of height of perfect mirror at the receiver positions, $x = 1$ and $x = 3$, for different SNRs.

promising technique to improve the system performance.

In order to generalize our proposed MDR with multiple PDs, we can arrange our proposed MDR isotropically to obtain the directivity and place both-side mirrors in the middle of multiple PDs. In Fig. 4, we show the example for the proposed MDR structure with four and six PDs. Fig. 4a and 4b show the case of extension to 2-dimensional MDR structure by using four PDs and installing the both-side mirror on both coordinates. In Fig. 4c and Fig. 4d, we utilize the design of receiver structure which is used to provide directivity in [7], [8]. This receiver geometry allows us to easily generalize the receiver structure with arbitrary number of PDs. We can install the one-side mirror inside of each PD in order to make directivity. The analysis on the channel matrix and system performance in the general MDR model will be our future work.

Finally, we also note that our proposed MDR can be applied to various scenarios although we here consider indoor VLC scenario. For instance, the proposed MDR might improve the system performance of multi-user detection in multiple access (MAC) free space optical MIMO channels and underwater wireless optical MIMO channels. In order to achieve better performance, our proposed MDR can be easily combined with the other previous receivers without modification.

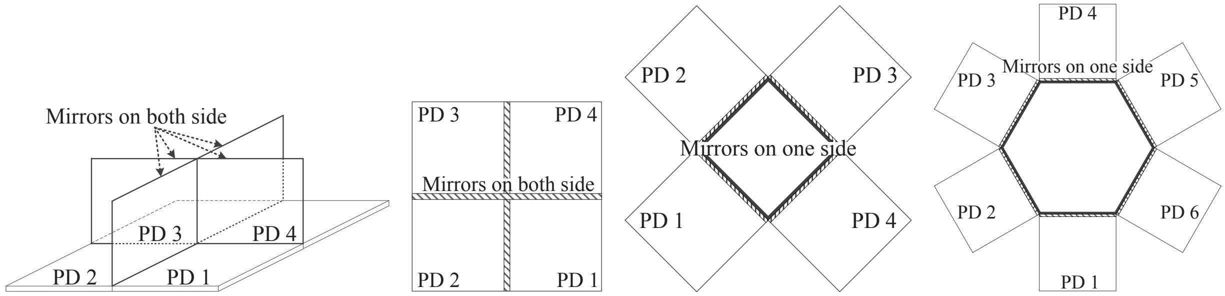

(a) Case I : MDR with four PDs

(b) Top view of Case I

(c) Case II : Alternative design of MDR with four PDs

(d) Case III : MDR with six PDs

Fig. 4. Generalization of the proposed MDR with multiple PDs. Hatching lines in the figure symbolize a mirror.

REFERENCES

[1] D. C. O'Brien, L. Zeng, H. L. Minh, G. Faulkner, J. W. Walewski, and S. Randel, "Visible light communications: challenges and possibilities," in *Proc. IEEE Personal, Indoor and Mobile Radio Communications (PIMRC 2008)*, Cannes, France, Sep. 2008.

[2] L. Zeng, D. O'Brien, H. Minh, G. Faulkner, K. Lee, D. Jung, Y. Oh, and E. T. Won, "High data rate multiple input multiple output (MIMO) optical wireless communications using white LED lighting," *IEEE J. Sel. Areas Commun.*, vol. 27, no. 9, pp. 1654–1662, Dec. 2009.

[3] A. H. Azhar, T. Tran, and D. O'Brien, "A Gigabit/s indoor wireless transmission using MIMO-OFDM visible-light communications," *IEEE Photon. Technol. Lett.*, vol. 25, no. 2, pp. 171–174, Jan. 2013.

[4] T. Q. Wang, Y. A. Sekercioglu, and J. Amstrong, "Analysis of an optical wireless receiver using a hemispherical lens with application in MIMO visible light communications," *J. Lightw. Technol.*, vol. 31, no. 11, pp. 1744–1754, Jun. 2013.

[5] T. Chen, L. Liu, B. Tu, Z. Zheng, and W. Hu, "High-spatial-diversity imaging receiver using fisheye lens for indoor MIMO VLCs," *IEEE Photon. Technol. Lett.*, vol. 26, no. 22, pp. 2260–2263, Nov. 2014.

[6] T. Fath and H. Haas, "Performance comparison of MIMO techniques for optical wireless communications in indoor environments," *IEEE Trans. Commun.*, vol. 61, no. 2, pp. 733–742, Feb. 2013.

[7] A. Nuwanpriya, S.-W. Ho, and C. S. Chen, "Indoor MIMO visible light communications: Novel angle diversity receivers for mobile users," *IEEE J. Sel. Areas Commun.*, vol. 33, no. 9, pp. 1780–1792, Sep. 2015.

[8] T. Q. Wang, R. J. Green, and J. Armstrong, "MIMO optical wireless communications using ACO-OFDM and a prism-array receiver," *IEEE J. Sel. Areas Commun.*, vol. 33, no. 9, pp. 1959–1971, Sep. 2015.

[9] S. Arnon, J. Barry, G. Karagiannidis, R. Schober, and M. Uysal, *Advanced Optical Wireless Communication Systems*. Cambridge University Press, 2013.

[10] I. S. Ansari, F. Yilmaz, and M.-S. Alouini, "Performance analysis of free-space optical links over Málaga turbulence channels with pointing errors," *IEEE Trans. Wireless Commun.*, vol. 15, no. 1, pp. 91–102, Jan. 2016.

[11] K.-H. Park, Y.-C. Ko, and M.-S. Alouini, "On the power and offset allocation for rate adaptation of spatial multiplexing in optical wireless MIMO channels," *IEEE Trans. Commun.*, vol. 61, no. 4, pp. 1535–1543, Apr. 2013.